Robust correlation receiver for distance estimation

Eriksson, Håkan; Börjesson, Per Ola; Ödling, Per; Holmer, Nils-Gunnar

Published in:
IEEE Transactions on Ultrasonics, Ferroelectrics and Frequency Control

DOI:
10.1109/58.308494

1994

A Robust Correlation Receiver for Distance Estimation

Håkan Eriksson, *Student Member, IEEE*, Per Ola Börjesson, *Member, IEEE*, Per Ödling, *Student Member, IEEE*, and Nils-Gunnar Holmer, *Member, IEEE*

Abstract—**Many methods for distance estimation, such as the ultrasonic pulse-echo method, involve the estimation of a *Time-of-Flight* (TOF). In this paper, a signal model is developed that, apart from the TOF, accounts for an unknown, linear frequency dependent distortion as well as for additive noise. We derive a TOF estimator for this model based on the criteria of *Maximum Likelihood*. The resulting receiver can be seen as an extension or generalization of the well known cross-correlation, or "matched filter", estimator described, e.g., by Nilsson in [12]. The novel receiver is found to be more robust against unknown pulse shape distortion than the cross-correlation estimator, giving less biased TOF estimates. Also, bias versus noise sensitivity can be controlled by proper model order selection.**

Index Terms—**Time-of-Flight, delay, estimation, narrow-band, ultrasound, robustness, pulse-echo method.**

I. Introduction

THE MOST widely used method for making ultrasonic measurements is the ultrasonic pulse-echo method, introduced by Pellam and Galt in 1946 [14]. It is used for the investigation and detection of changes in acoustic impedance. Applications can, for instance, be found in medical diagnostics [8] and nondestructive material testing [17]. An electric pulse is applied to an ultrasonic transducer which is in acoustic contact with the sample to be examined. The transducer converts the electric pulse into an acoustic pressure wave that is transmitted into the sample. Reflections will appear where the acoustic impedance changes, e.g., in surfaces between different tissues, and a pressure wave will be reflected to the transducer. The transducer receives and converts the reflected pressure wave into an electric signal. The objective is then to extract the desired information by analyzing this signal. In the case of distance estimation it is often assumed that the distance to be measured is proportional to the corresponding pressure wave flight time. This motivates our current interest in *Time-of-Flight* (TOF) estimation.

When performing TOF estimation the choice of system model is an intricate matter, also involving defining the TOF. In [12] the assumption that the received signal consists of nonoverlapping delayed and scaled replicas of a *known* "reference" echo renders the well-known cross-correlation, or "matched filter", estimator. The received signal is correlated with the reference signal and the position of the maximum of the absolute value of the correlation function yields the estimate of the TOF. This estimator is optimal in the sense that it is the *Maximum Likelihood* estimator of the TOF given additive white Gaussian noise with zero mean [18]. In general the shapes of the received echoes depend on many parameters, such as the locations and the geometry of the reflectors. Many methods for TOF estimation are based on the assumption that some feature of the received echoes is essentially invariant, for instance the shape [7], [12], the first zero crossing [3], [11], the amplitude peak of the echoes [15], the amplitude peak of the envelope of the echoes [19] or the initial part of the received echoes [5]. Then, in [3], [5], [7], [11], [15], [19] the positions in time of these features gives the TOF estimates. If the assumptions of invariance of the features in question are violated, the mentioned techniques for TOF estimation will be likely to produce biased estimates. In fact, the bias of the TOF estimate could well be greater than the standard deviation of the same, as we will exemplify in the sequel.

Throughout this paper we consider a propagation media containing only one reflector and the estimation of a single TOF. We address the problem of how to derive a receiver for TOF estimation when the shape of the received echo is unknown or uncertain.

The paper proceeds as follows. A method for modeling uncertainties in the shape of the received signal in narrow-band pulse-echo systems is presented in Section II. The modeling method is based on describing the received echo as a *known narrow-band* reference signal being distorted by an unknown linear and time-invariant system and corrupted with additive noise. This linear system is modeled in the frequency domain with a Taylor series expansion around the center frequency of the reference signal. The coefficients of the Taylor series expansion hold the uncertainty in the system. Inherent in the model is a definition of the TOF. In Section III we derive a TOF estimator, based on the ML criteria, using an Mth order truncation of the model derived in Section II. The estimation procedure consists of a joint estimation of the TOF and the $2M$ coefficients of the truncated Taylor expansion. In Section IV the estimator is simulated and its performance is compared with the performance of the cross-correlation estimator in terms of bias and standard deviation. Section V describes measurements where the cross-correlation estimator and the estimator of Section III is used to produce ultrasonic images for different model orders M. Finally, in Section VI comments on the results can be found.

Manuscript received June 30, 1993; revised February 16, 1994; accepted March 11, 1994.

H. Eriksson, P. O. Börjesson, and P. Ödling are with the Division of Signal Processing, Luleå University of Technology, S-971 87 Luleå, Sweden.

N.-G. Holmer is with the Department of Biomedical Engineering, Lund University, S-221 00 Lund, Sweden.

IEEE Log Number 9403351.

II. Linear Distortion of Narrowband Signals

Consider the situation described in Fig. 1. An unknown excitation signal is applied as an input to two unknown linear systems. The output signal from one of the systems, $s(t)$, is a real valued *known narrow-band* signal, henceforth called the reference signal. The output from the other system is denoted $y(t-\theta)$, where θ is the unknown delay to be estimated.

Assume that there exists an impulse response $h(t)$ so that the noiseless waveform

$$y(t-\theta) = (s * h)(t-\theta), \tag{1}$$

where $*$ denotes continuous time convolution and $h(t)$ is an unknown real valued impulse response representing linear distortion. Since the real valued reference signal is *narrow-band*, we write it as

$$s(t) = \Re\left\{e^{j2\pi f_0 t}\alpha(t)e^{j\beta(t)}\right\}, \tag{2}$$

where $\Re\{\cdot\}$ denotes the real part of its argument. The functions $\alpha(t)$ and $\beta(t)$ are real valued with the restriction that the Fourier transform of the complex envelope, $\alpha(t)e^{j\beta(t)}$, is zero outside the frequency interval $[-B, B]$, where $B \ll f_0$. We also assume that the complex envelope has finite energy, i.e., that $\alpha(t)e^{j\beta(t)} \in L_2(\mathcal{R}) = \{z(t) | \int |z(t)|^2 dt < \infty\}$.

Define $L_2^B(\mathcal{R})$ as the space of all signals in $L_2(\mathcal{R})$ whose Fourier transforms are zero outside the frequency interval $[-B, B]$. These signals will be referred to as baseband signals. Furthermore, due to the narrow-band assumption ($B \ll f_0$) on $s(t)$, it is convenient to define the subspace $L_2^{HF}(\mathcal{R})$ of $L_2(\mathcal{R})$ as the space of all signals in $L_2(\mathcal{R})$ whose Fourier transforms are zero outside the frequency intervals $[-f_0 - B, -f_0 + B]$ and $[f_0 - B, f_0 + B]$. By definition $\alpha(t)e^{j\beta(t)} \in L_2^B(\mathcal{R})$ and by construction $s(t) \in L_2^{HF}(\mathcal{R})$. Note that $s(t)$ can be any narrow-band signal having finite energy whose Fourier transform only has support in two intervals, symmetrically around $f = 0$ and not containing $f = 0$. These signals could typically be bandlimited ultrasonic pulse echo signals decaying fast enough in time to have finite energy.

Models related to (1) can be found in, e.g., [2], [4], [12]. The special case of (1) where $h(t)$ is modeled as the sum of weighted and delayed Dirac-delta functions has been extensively used in the context of TOF estimation, see, e.g., [12]. Recently in a paper by Boudreau and Kabal [2] a model for the purpose of TOF estimation is presented, allowing an unknown linear frequency dependent distortion in the delay path. The reference signal was there modeled as a broadband stochastic process for the tracking of a time varying TOF with an adaptive algorithm. A discrete time version of (1) is studied in [4], where the distortion is modeled as a linear stochastic system with a known Gaussian statistic.

A. An Mth Order Model of the Distorting System $h(t)$

Due to the narrow-band assumption on $s(t)$ we are only interested in the behaviour of $h(t)$ in the frequency intervals $[f_0 - B, f_0 + B]$ and $[-f_0 - B, -f_0 + B]$. Let $H(f)$ denote the Fourier transform of $h(t)$ and assume that $H(f)$ is M-times differentiable in an interval around $f = f_0$. Define $C_M(f)$ as

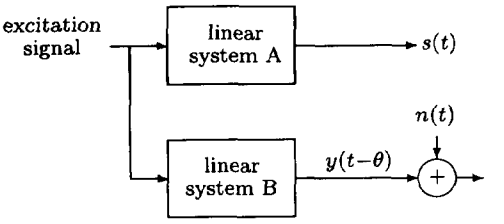

Fig. 1. A model of a measurement situation for TOF estimation.

the Taylor series expansion of $H(f)$ around $f_0 > 0$ with a remainder term of order M:

$$C_M(f) \triangleq \sum_{k=0}^{M-1} \frac{(f-f_0)^k}{k!} \frac{d^k}{df^k} H(f)\bigg|_{f=f_0}. \tag{3}$$

Now, let us define a function $H_M(f)$ such that $H_M(f) = C_M(f)$ for $f > 0$ and the inverse Fourier transform of $H_M(f)$ is real valued,

$$H_M(f) \triangleq C_M(f)U(f) + C_M^*(-f)U(-f), \tag{4}$$

where $U(f)$ denotes the unit step function and the superscript $*$ denotes the complex conjugate.

The system model $H_M(f)$ is then an Mth order model of $H(f)$, especially adapted for narrow-band signals with their center frequency equal to f_0. A similar reasoning by Papoulis can be found in [13, page 59] for baseband signals.

B. Evaluation of the Convolution $(s * h)(t)$

For the purpose of modeling the convolution $(s * h)(t)$ in (1), we define

$$y_M(t) \triangleq \mathcal{F}^{-1}\{\mathcal{F}\{s(t)\}H_M(f)\}, \tag{5}$$

where $\mathcal{F}\{\cdot\}$ denotes the Fourier transform and $\mathcal{F}^{-1}\{\cdot\}$ its inverse. By using the narrow-band representation of the reference signal in (2), it follows that

$$y_M(t) = \Re\left\{e^{j2\pi f_0 t} \sum_{k=0}^{M-1} (a_k + jb_k)g^{(k)}(t)\right\}, \tag{6}$$

where a_k and b_k are real valued coefficients given by

$$a_k + jb_k = \frac{1}{(j2\pi)^k k!} \frac{\partial^k H(f)}{\partial f^k}\bigg|_{f=f_0}, \tag{7}$$

and

$$g^{(k)}(t) = \frac{d^k}{dt^k}\left\{\alpha(t)e^{j\beta(t)}\right\}. \tag{8}$$

All $g^{(k)}(t)$ exist and have Fourier transforms that are zero outside the frequency interval $[-B, B]$ since the subspace $L_2^B(\mathcal{R})$ is closed under linear operations and $g^{(0)}(t)$ is analytic having derivatives of all orders in every point on $\mathcal{R}$.

We now have obtained a signal representation, (6)–(8), with the model order M to choose. Observe that the waveforms $\{g^{(k)}(t)\}_{k=0}^{M-1}$ are independent of the system $h(t)$ and that the coefficients $\{a_k, b_k\}_{k=0}^{M-1}$ are independent of the reference signal once the center frequency is given. Thus, the knowledge of the reference signal gives us a signal basis and the

coefficients $\{a_k, b_k\}_{k=0}^{M}$ hold the uncertainty in the shape of the waveform $y_M(t)$.

For the development of the estimator in Section III we need an orthogonal signal basis. Define the inner product $\langle \cdot, \cdot \rangle$ in $L_2(\mathcal{R})$ as

$$x, y \triangleq \int_{\mathcal{R}} x(t) y^*(t) dt, \tag{9}$$

and the norm $\|x\| \triangleq \langle x, x \rangle^{1/2}$. Since $g^{(0)}(t) \in L_2^B(\mathcal{R})$ it can be shown that the signal set $\{g^{(k)}\}_{k=0}^{M-1}$ spans an M-dimensional signal space Ω_M in $L_2^B(\mathcal{R})$. Let $\{z_k\}_{k=0}^{N-1}$ denote an orthonormal signal basis that spans Ω_N, for every N in $\{1, \ldots, M\}$, which ensures the signal basis $\{z_k\}_{k=0}^{M-1}$ to be in a specific order. This signal basis can, for instance, be obtained by applying Gram-Schmidt orthogonalization to $\{g^{(k)}\}_{k=0}^{M-1}$. Let us modulate the signal basis $\{z_k\}_{k=0}^{M-1}$ up to the frequency band of interest and define

$$\left.\begin{array}{rcl} \psi_k(t) & \triangleq & \sqrt{2}\Re\{z_k(t)e^{j2\pi f_0 t}\} \\ \tilde{\psi}_k(t) & \triangleq & \sqrt{2}\Im\{z_k(t)e^{j2\pi f_0 t}\} \end{array}\right\}, \; k = 0, 1, \ldots, M-1, \tag{10}$$

where $\Im\{\cdot\}$ denotes the imaginary part of its argument. Since the Fourier transform of z_k is narrow-band ($B \ll f_0$) and $\langle z_k, z_l \rangle = \delta_{kl}$ the function set $\{\psi_k, \tilde{\psi}_k\}_{k=0}^{M-1}$ is a real valued orthonormal basis of dimension $2M$ in $L_2^{HF}(\mathcal{R})$. The model signal $y_M(t)$ in (5) can then be expressed as a linear combination of $\{\psi_k, \tilde{\psi}_k\}_{k=0}^{M-1}$ according to

$$y_M(t) = \sum_{k=0}^{M-1} c_k \psi_k(t) + d_k \tilde{\psi}_k(t). \tag{11}$$

The unknown coefficients $\{c_k, d_k\}_{k=0}^{M-1}$ are the new coordinates for $\{a_k, b_k\}_{k=0}^{M-1}$ after the change of signal basis. The coefficients $\{c_k, d_k\}_{k=0}^{M-1}$ now hold the uncertainty in the shape of the waveform $y_M(t)$. Note that $\psi_0(t)$ is a normalized replica of the reference signal, i.e., $\psi_0(t) = s(t)/\|s\|$, and that $\psi_k(t)$ and $\tilde{\psi}_k(t)$ by construction form a Hilbert transform pair for all k in $\{0, \ldots, M-1\}$.

C. A Summary of the Signal Basis Design

In this section we have presented a method for modeling linear distortion of narrow-band signals. The analysis results in a signal representation consisting of an orthonormal signal basis. The design process for obtaining this signal basis can be summarized as follows:

- For $k = 0, 1, \ldots, M-1$, take the kth order derivative of the bandlimited complex envelope of the reference signal, see (8).
- Use for instance the Gram-Schmidt orthogonalization process to obtain a complex orthonormal baseband signal basis, $\{z_k\}_{k=0}^{M-1}$.
- Calculate the high frequency signal basis, $\{\psi_k(t), \tilde{\psi}_k(t)\}_{k=0}^{M-1}$, as described by (10).

In the case when $s(t)$ is acquired by a calibration or measurement procedure, the design process will be affected by noise. To reduce this effect, a band-pass filter matched to the bandwidth of $s(t)$ should be introduced when acquiring $s(t)$, thereby reducing the noise power. The design process is described in Fig. 2 where LP denotes an ideal low pass filter with a bandwidth equal to B, i.e., the bandwidth of $\alpha(t)e^{j\beta(t)}$.

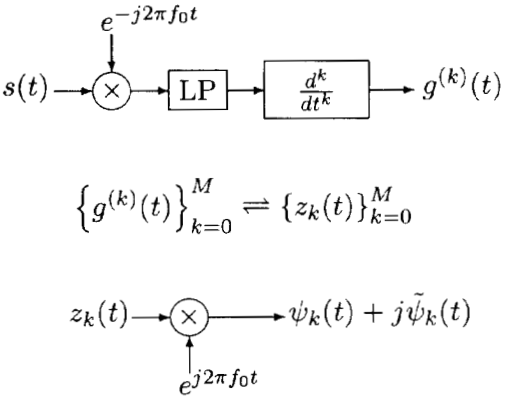

Fig. 2. A design structure for generating the signal basis $\{\psi_k(t), \tilde{\psi}_k(t)\}_{k=0}^{M-1}$.

III. Time of Flight Estimation

Consider the joint estimation of a single TOF and the coefficients describing the linear distortion. We model the received signal as

$$r(t) \triangleq y_M(t - \theta) + n(t), \tag{12}$$

where $y_M(\cdot)$ is given by the Mth order model (11) and $n(t)$ is an additive white Gaussian noise process, with zero mean and a power spectral density equal to $N_0/2$. The parameter θ is the TOF. With this definition of the TOF the shape of the waveform $y_M(\cdot)$ is allowed to vary, cf., [3], [5], [7], [11], [12], [15], [19].

To get a compact notation we rewrite $y_M(\cdot)$ of (11) as

$$y_M(t - \theta) = \mathbf{p}^T \psi(t - \theta), \tag{13}$$

where $\psi = [\psi_0, \ldots, \psi_{M-1}, \tilde{\psi}_0, \ldots, \tilde{\psi}_{M-1}]^T$ is a vector representation of the orthonormal signal basis and $\mathbf{p} = [c_0, \ldots, c_{M-1}, d_0, \ldots, d_{M-1}]^T$. With this notation we write the Signal to Noise Ratio (SNR) as

$$\text{SNR} \triangleq \frac{\|y_M\|^2}{N_0/2} = \frac{\mathbf{p}^T \mathbf{p}}{N_0/2}. \tag{14}$$

A. The ML Estimator

The estimation problem is to determine the unknown TOF θ when observing $\{r(t) \mid t \in \mathcal{I}\}$, where $\mathcal{I} = [T_1, T_2]$ is the observation interval ($T_1 < T_2$). Define the deterministic parameter vector

$$\mathbf{q} \triangleq \left[\theta, \mathbf{p}^T\right]^T \tag{15}$$

and denote the estimate of $\mathbf{q}$ as $\hat{\mathbf{q}} = [\hat{\theta}, \hat{\mathbf{p}}^T]^T$. The function

$$\begin{aligned} l(\mathbf{q} \mid r(t)) \; &= \tfrac{2}{N_0} \textstyle\int_{\mathcal{I}} r(t) y_M(t - \theta) dt \\ &\quad - \tfrac{1}{N_0} \textstyle\int_{\mathcal{I}} y_M^2(t - \theta) dt, \end{aligned} \tag{16}$$

is a log likelihood function for $\mathbf{q}$ given the observation $\{r(t) \mid t \in \mathcal{I}\}$, c.f. [18, p. 274]. Using (13), (16) can be written as

$$l(\mathbf{q} \mid r(t)) = \frac{2}{N_0}\mathbf{p}^T\mathbf{r}_\theta - \frac{1}{N_0}\mathbf{p}^T\mathbf{p} + \frac{1}{N_0}\mathbf{p}^T\mathbf{E}(\theta)\mathbf{p}, \quad (17)$$

where $\mathbf{r}_\theta$ is a vector resulting from $2M$ parallel correlations,

$$\mathbf{r}_\theta = \int_{\mathcal{I}} r(t)\psi(t-\theta)dt, \quad (18)$$

and where the matrix

$$\mathbf{E}(\theta) = \int_{\text{outside } \mathcal{I}} \psi(t-\theta)\psi^T(t-\theta)dt. \quad (19)$$

The only term involving the measurements $r(t)$ in (17) is the vector $\mathbf{r}_\theta$, where $\mathbf{r}_\theta$ is a sufficient statistic for the parameter vector $\mathbf{q}$.

For a given observation $\{r(t) \mid t \in \mathcal{I}\}$, the ML estimate of $\mathbf{q}$ is obtained by locating the global maximum of the log likelihood function $l(\mathbf{q} \mid r(t))$ with respect to $\mathbf{q}$. Let $\theta \in \mathcal{I}_\theta$, where $\mathcal{I}_\theta$ is an interval, or a set of intervals, on $\mathcal{R}$. If the observation interval $\mathcal{I}$ is chosen sufficiently large for $\psi_k(t-\theta)$ and $\tilde{\psi}_k(t-\theta)$ to have negligible energy outside $\mathcal{I}$ for all $\theta \in \mathcal{I}_\theta$, then, according to Schwarz's inequality, each element in $\mathbf{E}(\theta)$ is not greater than this negligible energy. Approximating $\mathbf{E}(\theta)$ with zero and completing the square in (17) we have

$$l(\mathbf{q} \mid r(t)) = -\frac{1}{N_0}(\mathbf{p}-\mathbf{r}_\theta)^T(\mathbf{p}-\mathbf{r}_\theta) + \frac{1}{N_0}\mathbf{r}_\theta^T\mathbf{r}_\theta. \quad (20)$$

For any given θ the maximum of $l(\mathbf{q} \mid r(t))$, with respect to $\mathbf{p}$, is given by $\mathbf{p} = \mathbf{r}_\theta$. Using $\mathbf{r}_\theta$ for $\mathbf{p}$ in (20), it follows that the location of the global maximum of $l(\mathbf{q} \mid r(t))$, with respect to $\mathbf{q}$ (resulting in an approximate ML estimate of $\mathbf{q}$), is given by

$$\begin{aligned} \widehat{\theta}_{ML}(\mathbf{r}) &= \arg\max_{\theta \in \mathcal{I}_\theta} \{x_M(\theta)\} \\ \widehat{\mathbf{p}}_{ML} &= \mathbf{r}_{\theta=\widehat{\theta}_{ML}} \end{aligned} \quad (21)$$

where

$$x_M(\theta) = \mathbf{r}_\theta^T\mathbf{r}_\theta. \quad (22)$$

Fig. 3 depicts a receiver structure for generating $x_M(t)$ from $r(t)$ according to (22). We henceforth refer to this receiver as the Mth *order extended correlation receiver*. Note that an ML estimator, in its general form, need not to be unbiased. This also applies to the Mth order extended correlation receiver.

B. A Comparison With the Cross-Correlation Estimator

The cross-correlation, or "matched filter", estimator of [12] is derived using the Maximum Likelihood criterion and assumptions of additive white Gaussian noise and perfect knowledge of the linear distortion, except for an unknown amplification factor. The received signal is correlated with a *known* waveform corresponding to $y_M(t)$ in (16), and the position of the maximum of the absolute value of the correlation function yields the estimate of the TOF. This receiver, when applied to a situation where the assumptions are valid, is unbiased and has a performance that meets the Cramér-Rao lower bound for high SNR's, see, e.g., [9] and the references therein. For low SNR's the cross-correlation estimator will suffer from a threshold effect when applied to narrow-band signals in the sense that the performance decreases rapidly with decreasing SNR below a certain SNR [9].

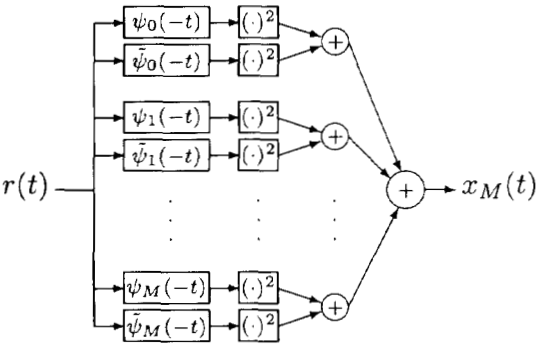

Fig. 3. A receiver structure for generating $x_M(t)$ according to (22). The function $r(t)$ is set to zero outside the observation interval $\mathcal{I}$ due to the implementation of the correlators as filters.

The Mth order extended correlation receiver can be described as a cross-correlation estimator that first estimates the received waveform $y_M(t-\theta)$ and then correlates the received signal $r(t)$ with this estimate. This can be seen, cf. [18, p. 354], by substituting the right-hand side of (18) for one of the $\mathbf{r}_\theta$'s in (22), giving

$$x_M(\theta) = \int_{\mathcal{I}} r(t)\widehat{y}_M(t-\theta)dt. \quad (23)$$

where

$$\widehat{y}_M(t-\theta) = \mathbf{r}_\theta^T\psi(t-\theta). \quad (24)$$

The function $\widehat{y}_M(t-\theta)$ can be interpreted as an estimate of $y_M(t-\theta)$ for a given θ, cf. (13) with $\mathbf{p}$ estimated by $\mathbf{r}_\theta$.

IV. Estimation Example

Let us investigate the influence of the model order M on the bias and the standard deviation of the TOF estimate by means of Monte Carlo simulations. We compare the performance of the cross-correlation estimator and the performance of the Mth order extended correlation receiver for different values of the model order M and various SNR's.

In these simulations the reference signal $s(t)$ is given by (2) with $\beta(t) = 0$ and $\alpha(t)$ as a Hanning window in the frequency domain. With a Hanning window of bandwidth B, the Fourier transform of $\alpha(t)$ becomes

$$\mathcal{F}\{\alpha(t)\} = \begin{cases} 1/2 + 1/2\cos\left(\frac{\pi f}{B}\right), & |f| < B \\ 0, & \text{otherwise} \end{cases} \quad (25)$$

The center frequency of the reference signal was chosen as $f_0 = 2B$ Hz. In all of these simulations the cross-correlation estimator is matched to the reference signal. For each estimator and every integer value of SNR, the TOF of one thousand echoes has been estimated.

In Figs. 5–6 the absolute value of the bias and the standard deviation of the receivers are shown for a case when the received signal has been subjected to a specific "unknown"

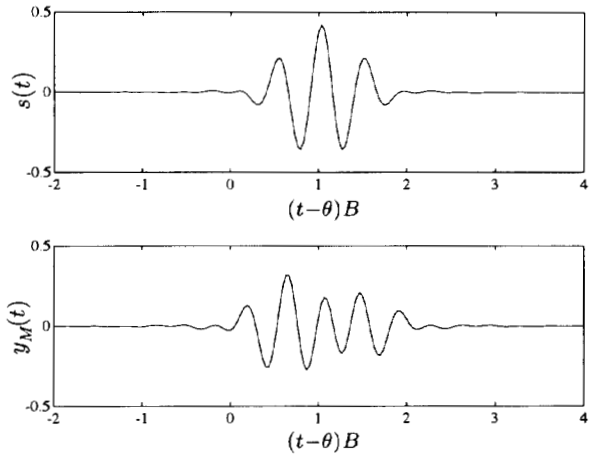

Fig. 4. The reference signal $s(t)$ and the model $y_M(t)$ in (11) in the case when $M = 2$ and $\mathbf{p} = [1/3, 2/3, 1/3, 1/6]^T$.

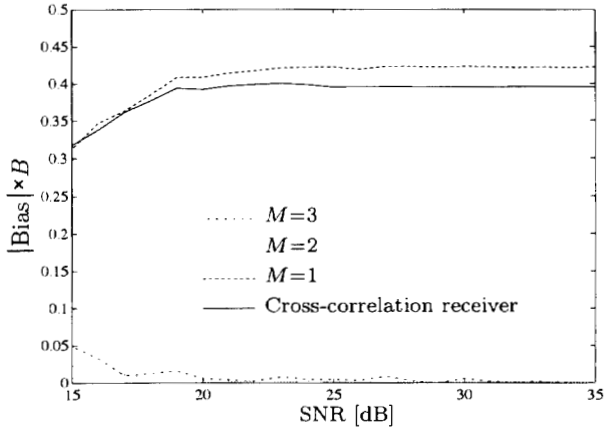

Fig. 5. The absolute value of the estimated and normalized bias of the receivers plotted versus SNR when a specific frequency dependent linear distortion is present.

linear distortion. Note that the bias and the standard deviation in the figures have been normalized with $1/B$. The distortion is described by $y_M(t)$ in (13), with $M = 2$ and $\mathbf{p} = [1/3, 2/3, 1/3, 1/6]^T$. Fig. 4 shows $y_M(t)$ together with the reference signal $s(t)$. In Fig. 7 the standard deviation of the receivers is given for the case when no frequency dependent linear distortion is present, i.e., $y_M(t) = as(t)$ where a is an unknown constant. The bias was, in this case, almost equal to zero for all receivers.

We make the following observations. When linear distortion is present the bias of the cross-correlation estimator can be much greater than the standard deviation of the same. The TOF estimates of the first-order extended correlation receiver are almost as biased as the estimates of the cross-correlation estimator. As expected, since the linear distortion is generated with $M = 2$, the second-order extended correlation receiver has very little bias compared with the cross-correlation estimator. It can be noted that the variance of the estimates in general increases with the model order M, especially when no linear distortion is present. An exception can be seen in Fig. 6 for SNR's less than 22 dB. Here both the bias and the variance of the TOF estimate are small for the second-order

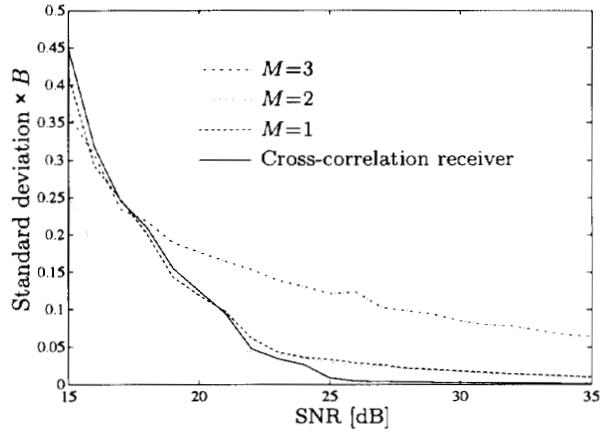

Fig. 6. The estimated normalized standard deviation of the receivers plotted versus SNR when a specific frequency dependent linear distortion is present.

extended correlation receiver whose model order is matched to the linear distortion.

From these and other simulations we draw the following conclusions. The cross-correlation estimator may give biased estimates when linear distortion not accounted for is present and the error due to bias can be more severe than the error caused by the additive white Gaussian noise. By using the Mth order extended correlation receiver the bias caused by linear distortion can be reduced. Robustness against linear distortion of the shape of the received pulse can be traded for noise sensitivity by increasing the model order M.

V. Ultrasonic Measurements

In this section we present results from using an experimental ultrasonic system to produce relief pictures of a surface structure by estimating the TOF of echoes reflecting from different points on the surface. This is a typical example of when it is difficult to choose a specific waveform as the reference signal for the cross-correlation estimator.

A. Measurement Setup

Experiments were carried out by scanning over a Swedish five crown coin in a 100 by 100 point grid, with a distance of 0.3 mm between adjacent points. The coupling medium between the transducer and the surface was air at room temperature. A circular transducer with a radius of 10.5 mm and a nominal frequency of 1 MHz was used. (The wavelength in air at room temperature is approximately 0.3 mm). The transducer was a focused transducer acoustically adapted to air, with a focal distance of 25 mm. It was designed by H. W. Persson for the investigation presented in [16]. The data were acquired with a LeCroy 9430 sampling oscilloscope. The sampling rate was chosen as 5.5 MHz and the sampling was synchronized with the transmitter by the use of an external crystal oscillator. The distance between the transducer and the surface of the coin was equal to the focal distance of the transducer.

B. Signal Processing and Measurements

A reference echo was acquired for the design of the signal basis $\{\psi_k, \tilde{\psi}_k\}_{k=0}^{M-1}$, i.e., the receiver filter bank in Fig. 3,

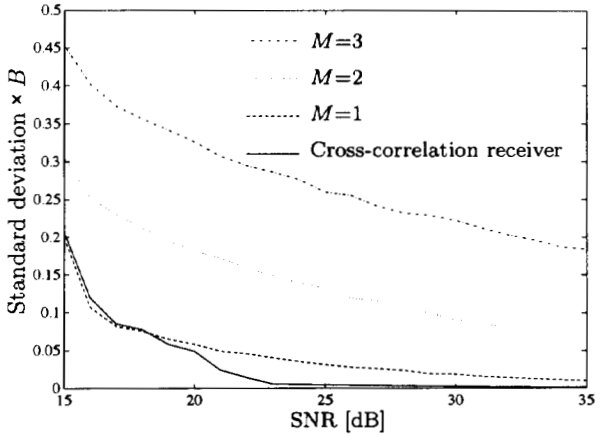

Fig. 7. The estimated normalized standard deviation of the receivers plotted versus SNR when *no* frequency dependent linear distortion is present.

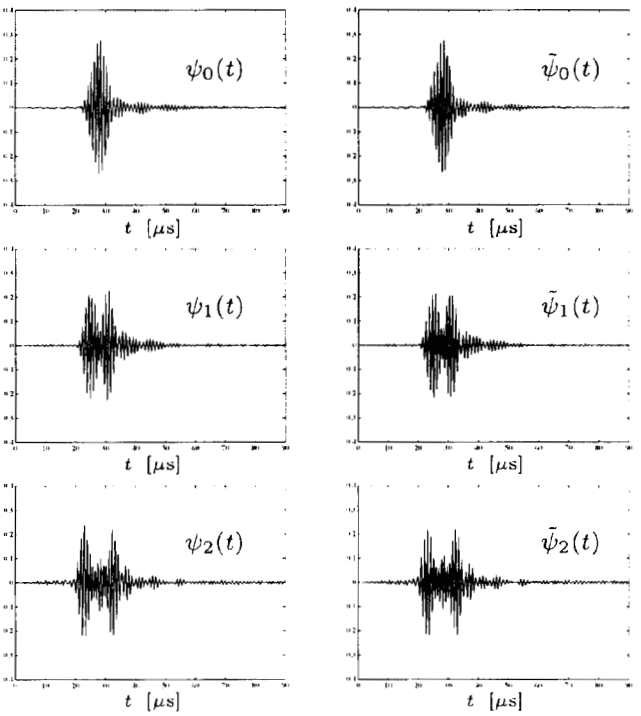

Fig. 8. The basis $\{\psi_k(t), \tilde{\psi}_k(t)\}_{k=0}^{2}$ corresponding to the acquired reference signal.

by letting the acoustic wave be reflected on the flat tip of a cut steel needle with a diameter of 1 mm, placed in the focal point of the transducer, cf., [10]. When acquiring the reference signal an averaging over 1000 B-scans was performed. The design process, described in Section II, Fig. 2, was then used to generate the signal set $\{\psi_k(t), \tilde{\psi}_k(t)\}_{k=0}^{M-1}$ for $M = 3$, see Fig. 8. As mentioned before the signal $\psi_0(t)$ is identical to the normalized reference signal. The reference signal is also illustrated in Fig. 9 and compared with the features on the surface of the coin.

The Mth order extended correlation receiver, (21)–(22), and the cross-correlation estimator were used to estimate the TOF for each point in the 100 by 100 point grid. Fig. 10 shows the result when the cross-correlation estimator matched to the

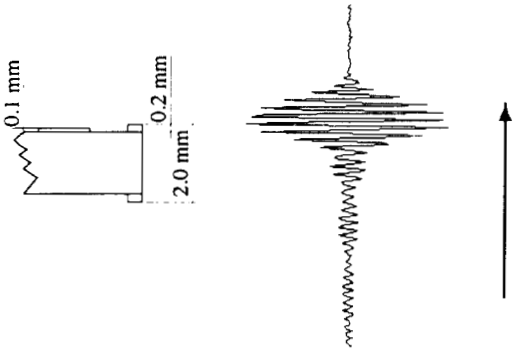

Fig. 9. The proportions of the features on the surface of the coin in comparison with the length of the reference signal.

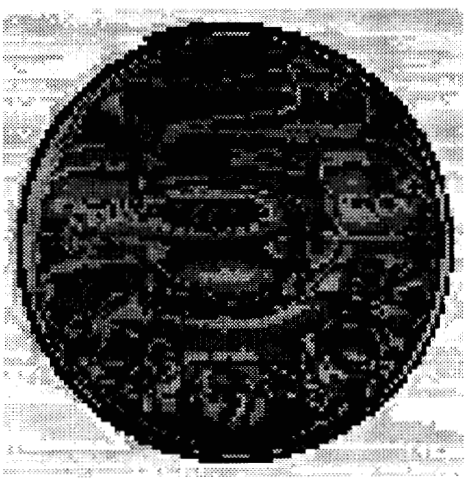

Fig. 10. A grey scale picture of a Swedish five crown coin, generated with the cross-correlation estimator matched to the reference signal $s(t)$.

reference signal $s(t)$ was used. Figs. 11–13 show the results when the Mth order extended correlation receiver was used with $M \in \{1, 2, 3\}$, respectively. All figures are derived from the same measured data.

In the grey-scale pictures the brightness of each pixel increases with the TOF. No post-processing has been performed to the data, except for a histogram normalization of the grey-scale level thresholds in the grey-scale pictures.

The SNR, when defined as in (14), varies from point to point in the grid, since the reflected signal energy depends on, e.g., the angle of the reflecting surface. Therefore, no SNR is presented in the figures. The SNR was though well above the threshold region [9] for the cross-correlation estimator (SNR $>$ 30 dB).

C. Comments on the Measurements

In the estimation examples presented the image corresponding to $M = 1$, Fig. 11, shows a significant improvement in quality compared to the image corresponding to the cross-correlation estimator, Fig. 10. The performance of the cross-correlation estimator is apparently sensitive to shape changes in the received waveform. The errors in the picture are mainly due to bias, since the SNR is high, and can for that reason not be removed by averaging repeated measurements. When

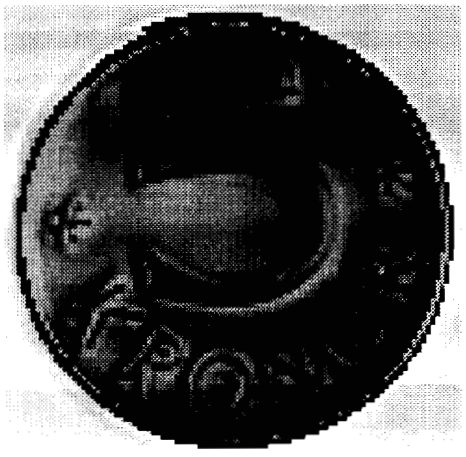

Fig. 11. A grey scale picture of a Swedish five crown coin, generated using the first-order extended correlation receiver.

Fig. 12. A grey scale picture of a Swedish five crown coin, generated using the second-order extended correlation receiver.

applying the receiver with $M = 3$ (Fig. 13) the disturbances due to the additive noise seem to dominate over the effects due to model errors. For this measurement situation the choices $M = 1$ and $M = 2$ appear to be the most appropriate.

The choice and the acquisition of the reference signal is a delicate matter, see, e.g., [6]. In this investigation we have used the echo from a cut needle located in the focal point of the transducer. We have not found any reference signal that gives the cross-correlation estimator a noticeable better performance in the presented measurement situation. However, other reference echoes could be used, for instance an echo from a flat surface where total reflection occurs, giving similar images.

VI. Conclusion

This paper treats the problem of how to design a receiver for TOF estimation when the received signal has been subjected to an unknown linear distortion. Based on a narrow-band assumption on the interrogation pulse, a model of the received signal incorporating unknown linear frequency dependent distortion has been presented together with a TOF estimator based on the criteria of *Maximum Likelihood*. This ML estimator can be seen as an extension or generalization of the cross-correlation estimator [12], and is referred to as the extended Mth order correlation receiver. The receiver can be implemented as a correlation receiver using a filter bank consisting of $2M$ parallel filters.

Simulations have shown that the performance of the cross-correlation receiver is sensitive to the choice of reference signal. The bias of the TOF estimate can be large compared with the standard deviation. By using the Mth order extended correlation receiver the bias caused by linear distortion can be reduced. In the presented ultrasonic measurements we observe that the Mth order extended correlation receiver achieves robustness against pulse shape distortion at the cost of increased noise sensitivity. By increasing the model order the tendency of bias in the TOF estimate can be traded for variance.

In this paper we only examine the case of estimating a single TOF. The receiver could be extended to estimating multiple TOF's, possibly with the exception of closely spaced echoes.

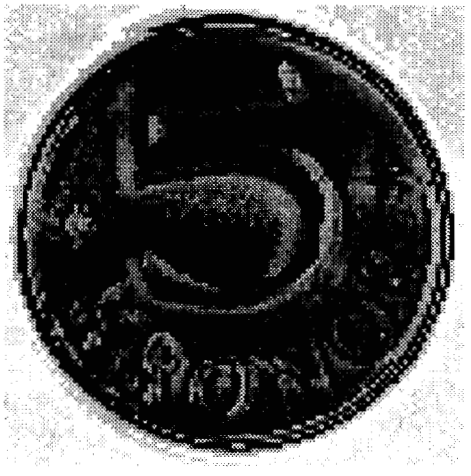

Fig. 13. A grey scale picture of a Swedish five crown coin, generated using the third-order extended correlation receiver.

We would like to point out that although this investigation is focused on ultrasound applications, the model presented only presumes a narrow-band pulse being distorted by a linear time-invariant system. Such conditions could also be present in other application areas.

References

[1] P. O. Börjesson, O. Pahlm, L. Sörnmo, and M.-E. Nygårds, "Adaptive QRS detection based on maximum *a posteriori* estimation," *IEEE Trans. Biomed. Eng.*, vol. 29, no. 5, pp. 341–351, 1982.

[2] D. Boudreau and P. Kabal, "Joint time-delay estimation and adaptive recursive least squares filtering," *IEEE Trans. Signal Process.*, vol. 41, no. 2, pp. 592–601, 1993.

[3] T. Bowen, W. G. Conner, R. L. Nasoni, A. E. Pifer, and R. R. Sholes, "Measurement of the temperature dependence of the velocity of ultrasound in soft tissue," in M. Linzer, Ed., *Ultrasonic Tissue Characterization II, NBS Special Publication*, vol. 525, U.S. Govt. Print. Office, 1979, pp. 57–61.

[4] H. Eriksson, P. Ödling, and P. O. Börjesson, "Simultaneous time of flight and channel estimation using a stochastic channel model," in *Radio Vetenskaplig Konferens RVK-93, Sammanfattning av Posters och Föredrag*, Lund, Sweden, April 1993, pp. 43–46.

[5] J. F. Greenleaf, S. A. Johnsson, W. F. Samayoa, and F. A. Duck, "Two-dimensional acoustic velocity distribution in tissues using an algebraic

reconstruction technique," in *Proc. Ultrason. Int. Conf.*, London, March 1975, pp. 190–195.
[6] A. Grennberg and M. Sandell, "Experimental determination of the ultrasonic echo from a pointlike reflector using a tomographic approach," in *Proc. 1992 Ultrason. Symp.*, Tuscon, AZ, Oct. 1992, pp. 639–642.
[7] V. N. Gupta, P. K. Baghat, and A. M. Fried, "Estimating ultrasound propagation velocity in tissue from unwrapping phase spectra," *Ultrason. Imaging*, no. 2, pp. 223–231, 1980.
[8] C. R. Hill, *Physical Principles of Medical Ultrasonics*. Chichester: Ellis Horwood Ltd., 1986.
[9] J. P. Ianiello, "Time delay estimation via cross-correlation in the presence of large estimation errors," *IEEE Trans. Acoust., Speech and Signal Process.*, vol. 30, no. 6, pp. 998–1003, 1982.
[10] J. A. Jensen, "A model for the propagation and scattering of ultrasound in tissue," *J. Acoust. Soc. Amer.*, vol. 89, no. 1, pp. 182–190, 1991.
[11] F. W. Kremkau, R. W. Barnes, and P. McGraw, "Ultrasonic attenuation and propagation in normal human brain," *J. Acoust. Soc. Amer.*, vol. 70, no. 1, pp. 29–38, 1981.
[12] N. J. Nilsson, "On the optimum range resolution of radar signals in noise," *IRE Trans. Inform. Theory*, vol. 32, no. 7, pp. 245–253, 1961.
[13] A. Papoulis, *The Fourier Integral and its Applications*. New York: McGraw-Hill, 1962.
[14] J. R. Pellam and J. K. Galt, "Ultrasonic propagation in liquids: I. Application of pulse technique to velocity and absorbation measurement at 15 megacycles," *J. Chemical Phys.*, vol. 14, no. 10, pp. 608–615, 1946.
[15] M. Ragozzino, "Analysis of the error in measurement of ultrasound speed in tissue due to waveform deformation by frequency-dependent attenuation," *Ultrason.*, no. 12, pp. 135–138, May 1981.
[16] N. Sundström, P. O. Börjesson, N.-G. Holmer, L. Olsson, and H. W. Persson, "Registration of surface structures using airborne focused ultrasound," *Ultrasound in Med. and Bio.*, vol. 17, no. 5, pp. 513–518, 1991.
[17] R. N. Thurston and A. D. Pierce, *Ultrasonic Measurement Methods*. San Diego, CA: Academic, 1990.
[18] H. L. van Trees, *Detection, Estimation, and Modulation Theory, Part I*. New York: Wiley, 1968.
[19] V. A. Verhoef, M. J. T. M. Clostermans, and J. M. Thijssen, "Diffraction and dispersion effects on the estimation of ultrasound attenuation and velocity in biological tissues," *IEEE Trans. Biomed. Eng.*, vol. 32, no. 7, pp. 521–529, 1985.

Håkan Eriksson was born in Stockholm, Sweden, in 1964. He received the M.Sc. degree in computer science from the Department of Computer Science and Electrical Engineering at Luleå University of Technology, Luleå, Sweden.

In July 1989, he began working towards the Ph.D. degree at the Division of Signal Processing at Luleå University of Technology. He presented his licentiate thesis on "Modelling of Waveform Deformation and Time-of-Flight Estimation" in June 1993. His current research involves parameter estimation in ultrasound signals and the properties of reduced complexity digital receivers.

Per Ola Börjesson was born in Karlshamn, Sweden in 1945. He received the M.Sc. degree in electrical engineering in 1970 and the Ph.D. degree in telecommunication theory in 1980, both from Lund Institute of Technology (LTH), Lund, Sweden. In 1983 he received the degree of Docent in Telecommunication Theory.

Since 1988 he has been Professor of Signal Processing at Luleå University of Technology. His primary research interest is the development of signal processing algorithms based on stochastic models, and their applications in telecommunications and biomedical engineering.

Per Ödling was born in Örnsköldsvik, Sweden, in 1966. He received the M.Sc. degree in 1989 and the Techn. Lic. degree in 1993, both from Luleå University of Technology, Sweden.

Currently, he is a Ph.D. student at the Division of Signal Processing, Luleå University of Technology. His research interests include the signal processing aspects of receivers used in telecommunications and receivers used in ultrasonics.

Nils-Gunnar Holmer was born in 1943 in Malmö, Sweden. He received the M.Sc. degree in electrical engineering 1968 and the Techn. Lic. degree in 1971, both from the Lund Institute of Technology. In 1978 he received the Ph.D. degree with a doctoral thesis entitled "New methods in medical ultrasound".

In 1981 he was accepted as an unpaid associate professor in electrical measurements at the Lund Institute of Technology. During 1973–1975 he was employed at the Department of Food Engineering where he designed and constructed measurement instruments for physical and chemical analysis. In 1975 he was with the Department of Biomedical Engineering, Malmö General Hospital as Vice Head of the department. In 1982 he became the Head of the Department of Biomedical Engineering at the Lund University Hospital. In 1986 he was appointed Professor of Biomedical Engineering at the University of Lund and in 1991 became the Supervising Chairman of the Biomedical Engineering Organization at Malmöhus County Council, which consists of five hospitals.